

Supporting Information for:

Improving the photoresponsivity and reducing the persistent
photocurrent effect of visible-light ZnO/quantum-dot
phototransistors via a TiO₂ layer

Byung Jun Kim^a, Sungho Park^a, Tae Yeon Kim^a, Eui Young Jung^a, Jong-Am Hong^b, Beom-Su
Kim^b, Woojin Jeon^a, Yongsup Park^b, and Seong Jun Kang^{a,*}

^a Department of Advanced Materials Engineering for Information and Electronics, Kyung Hee
University, Yongin 17101, Republic of Korea

^b Department of Physics and Research Institute for Basic Sciences, Kyung Hee University, Seoul
02447, Republic of Korea.

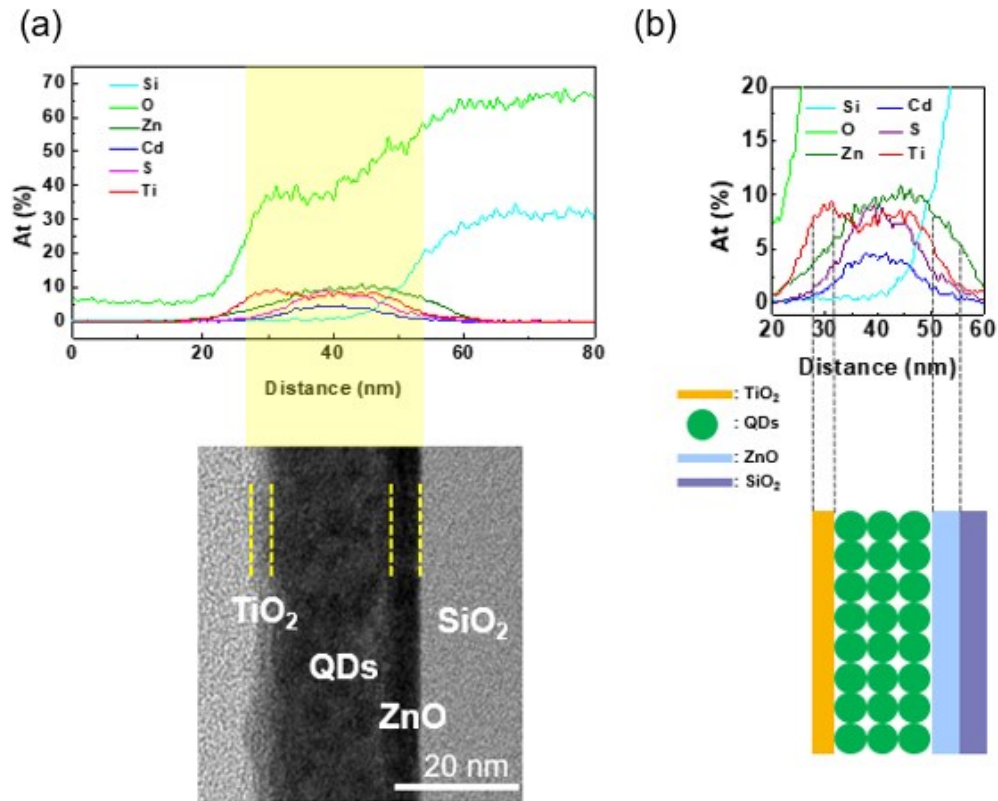


Figure S1. (a) Energy-dispersive spectroscopy (EDS) image from to SiO₂ to TiO₂. (b) EDS image of the ZnO/QDs/TiO₂ structure, in detail.

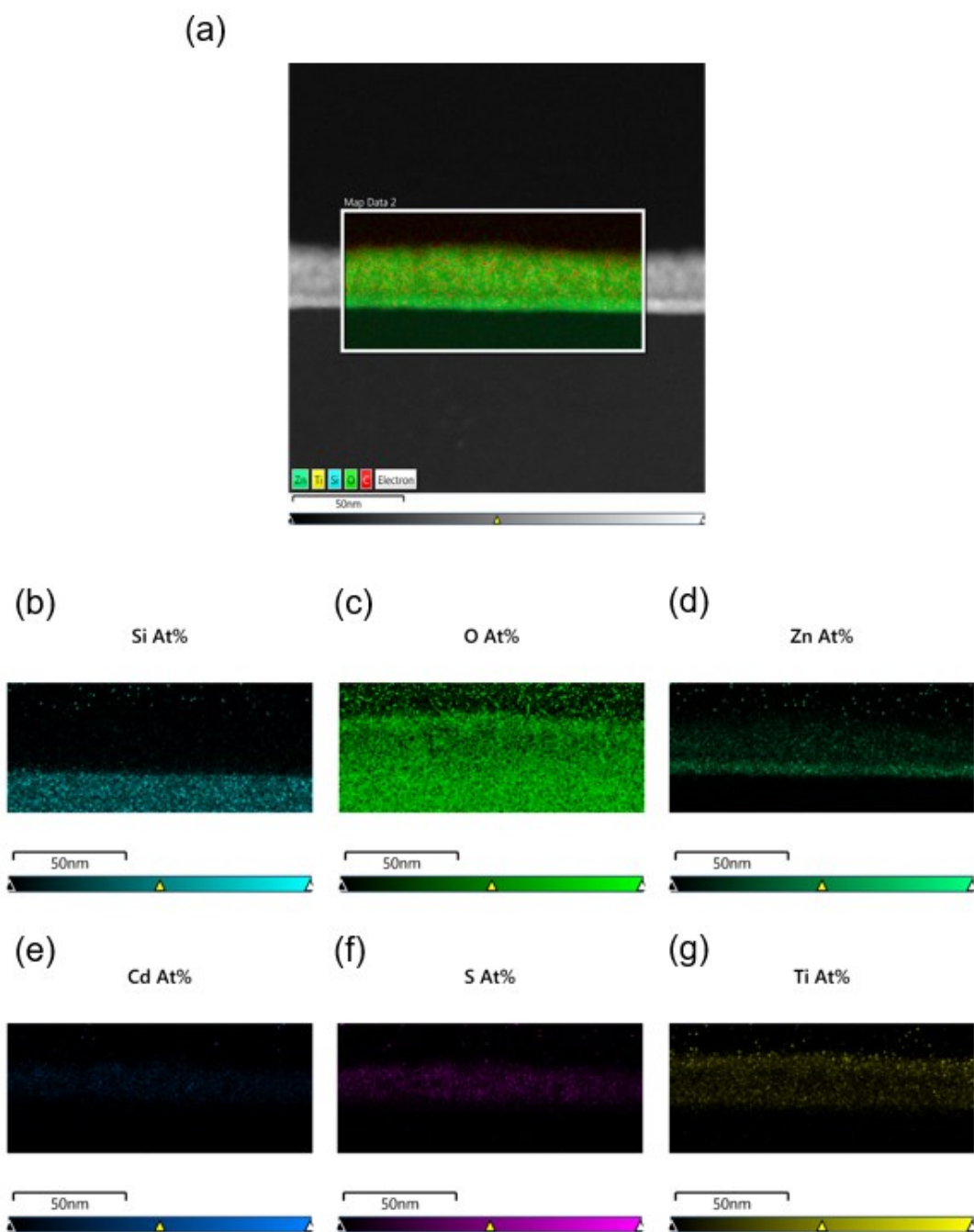


Figure S2. (a) Energy-dispersive X-ray spectroscopy (EDX) profile in the structure of ZnO/QDs/TiO₂. EDX profiles of ZnO/QDs/TiO₂ for the six detected elements; (b)-(g) Si, O, Zn, Cd, S, and Ti.

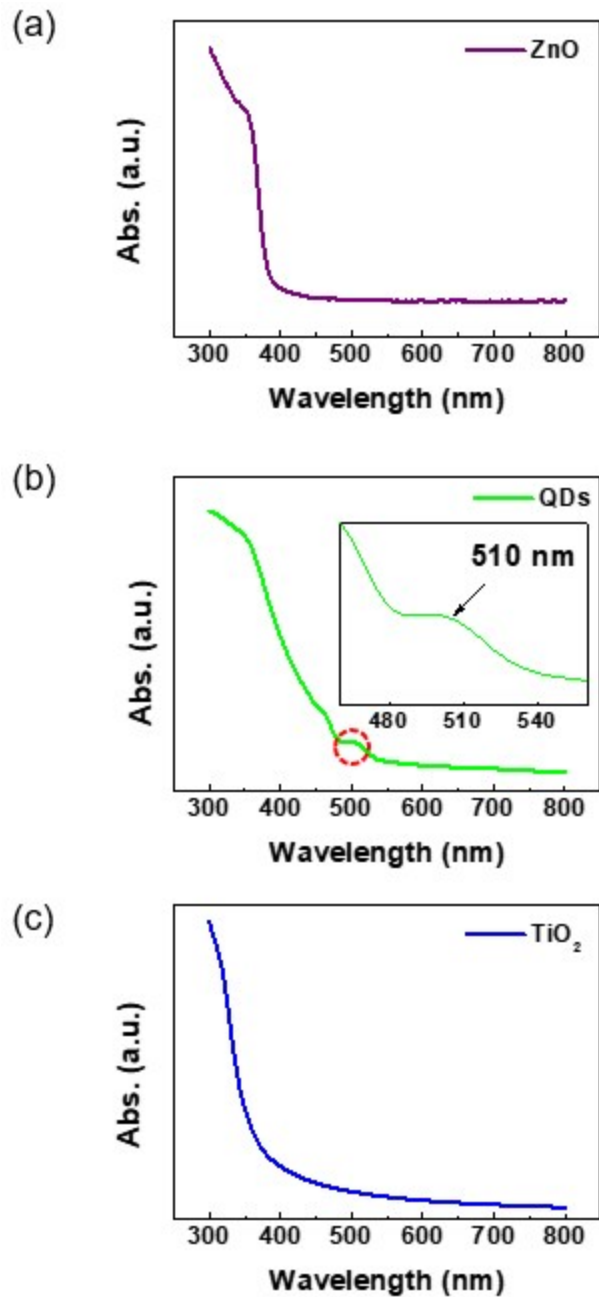


Figure S3. Absorption spectra of (a) ZnO, (b) QDs, and (c) TiO₂ film. The inset shows the absorption spectra from 480 to 540 nm in (b).

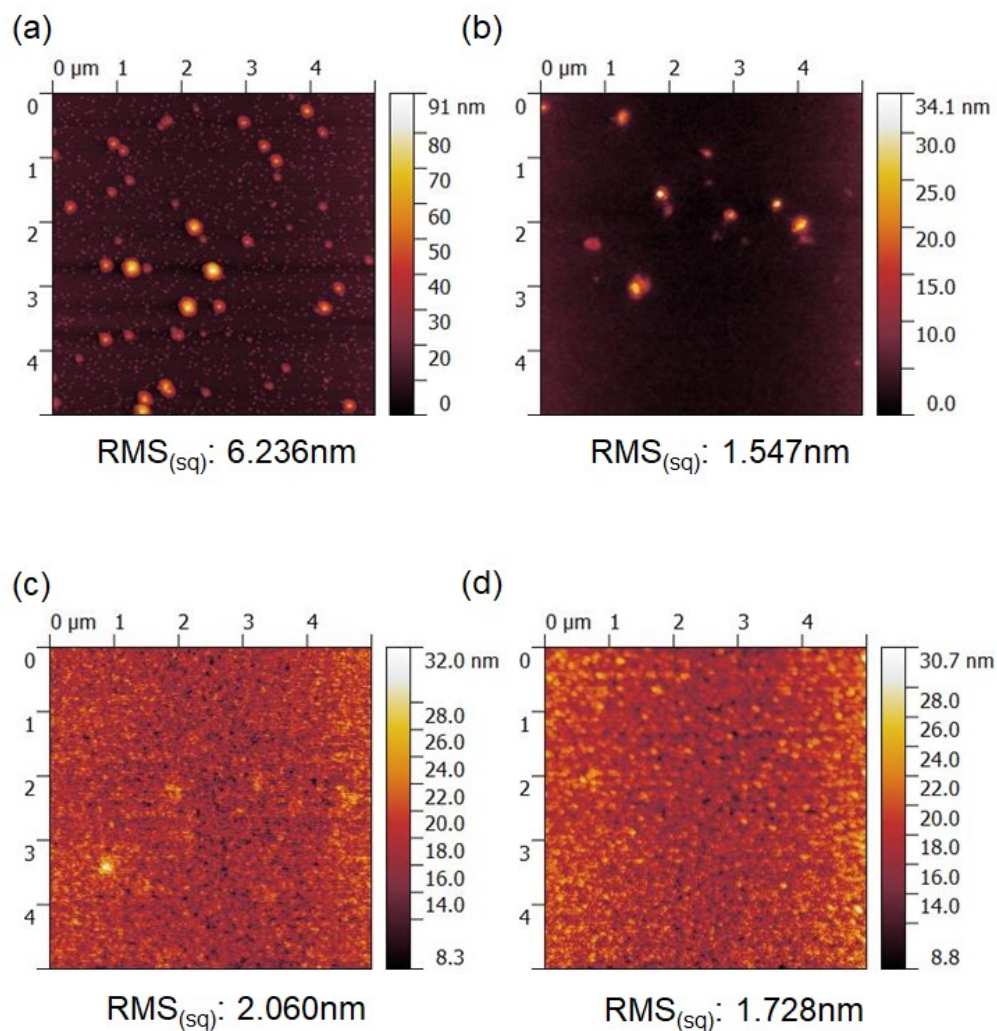


Figure S4. AFM The topography profiles of (a) SiO_2 (b) SiO_2/ZnO (c) $\text{SiO}_2/\text{ZnO}/\text{QDs}$ (d) $\text{SiO}_2/\text{ZnO}/\text{QDs}/\text{TiO}_2$ films. There is variation of RMS roughness with each stacked film. TiO_2 capping layer can enhance the surface of conventional ZnO/QDs structure through RMS roughness.

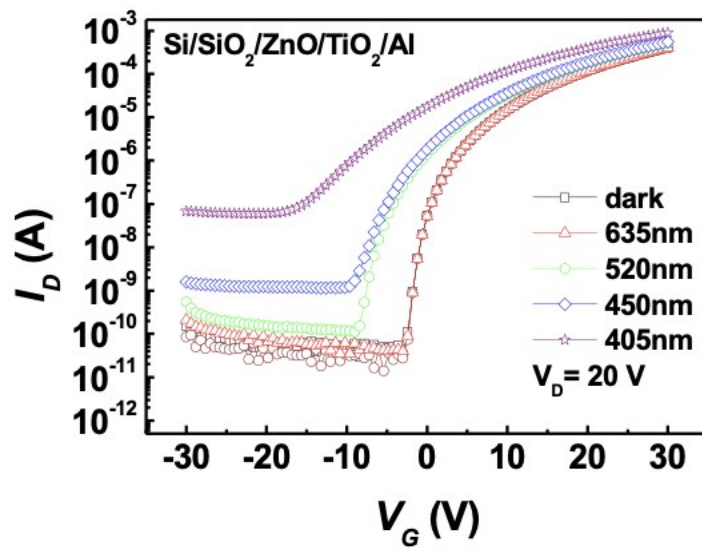


Figure S5. Transfer characteristics of the (a) ZnO/TiO₂ and (b) ZnO/QDs/TiO₂ TFTs under the illumination with various wavelengths.

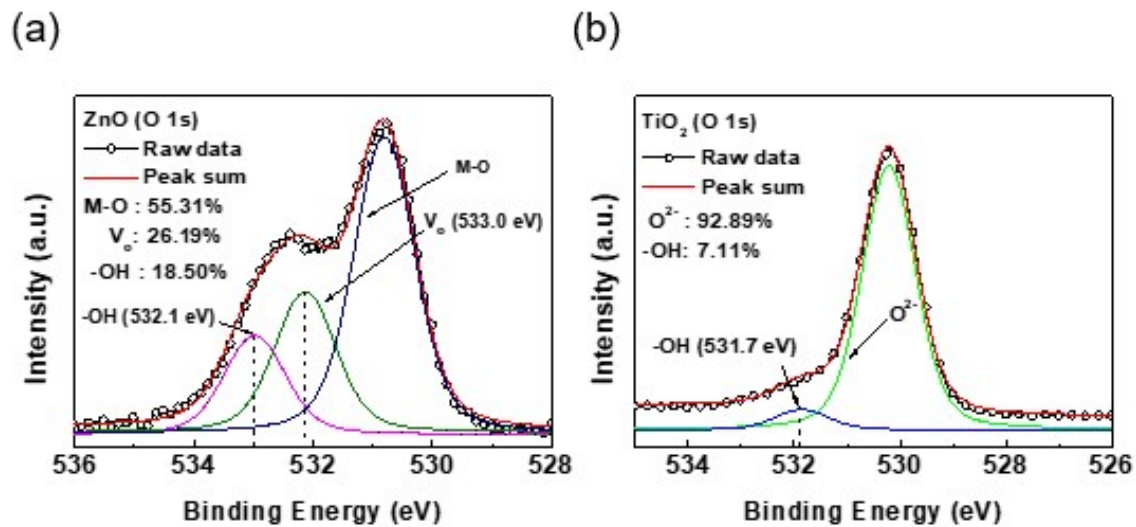


Figure S6. XPS O 1s spectra of the (a) ZnO and (b) TiO₂.

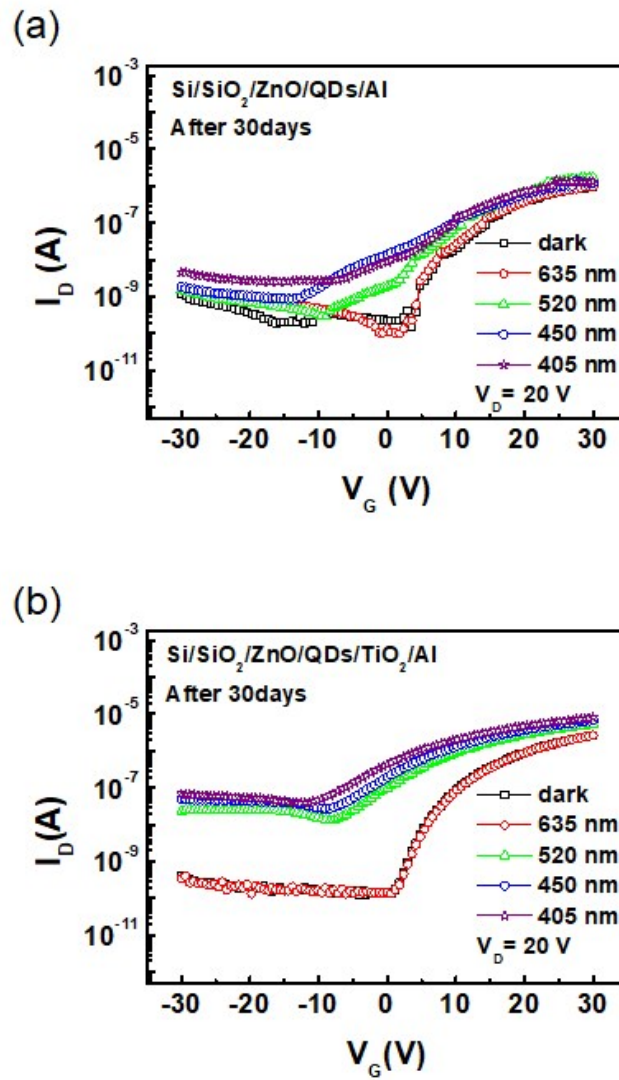


Figure S7. Long-term stability of the (a) ZnO/QDs and (b) ZnO/QDs/TiO₂ phototransistors after 30days.

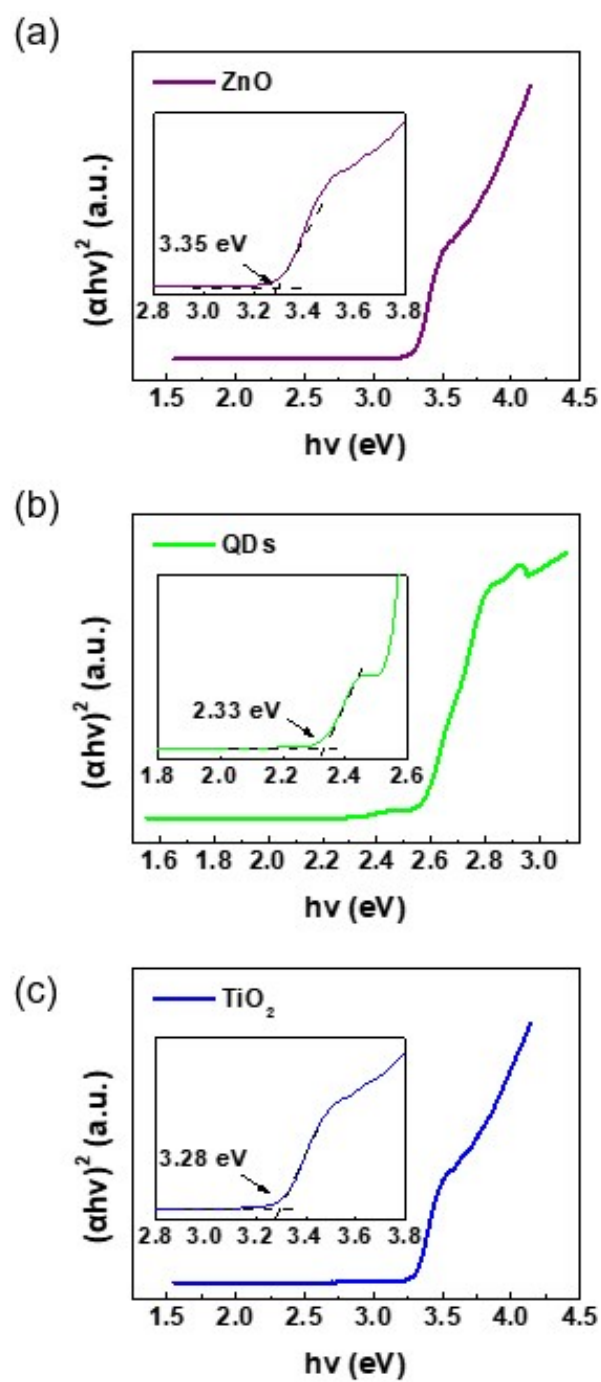


Figure S8. Tauc plots fitted by the $(\alpha h\nu)^2$ values of (a) ZnO and (b) QDs, and (c) TiO_2 film. The inset shows tauc plots with narrow ranges of each film.

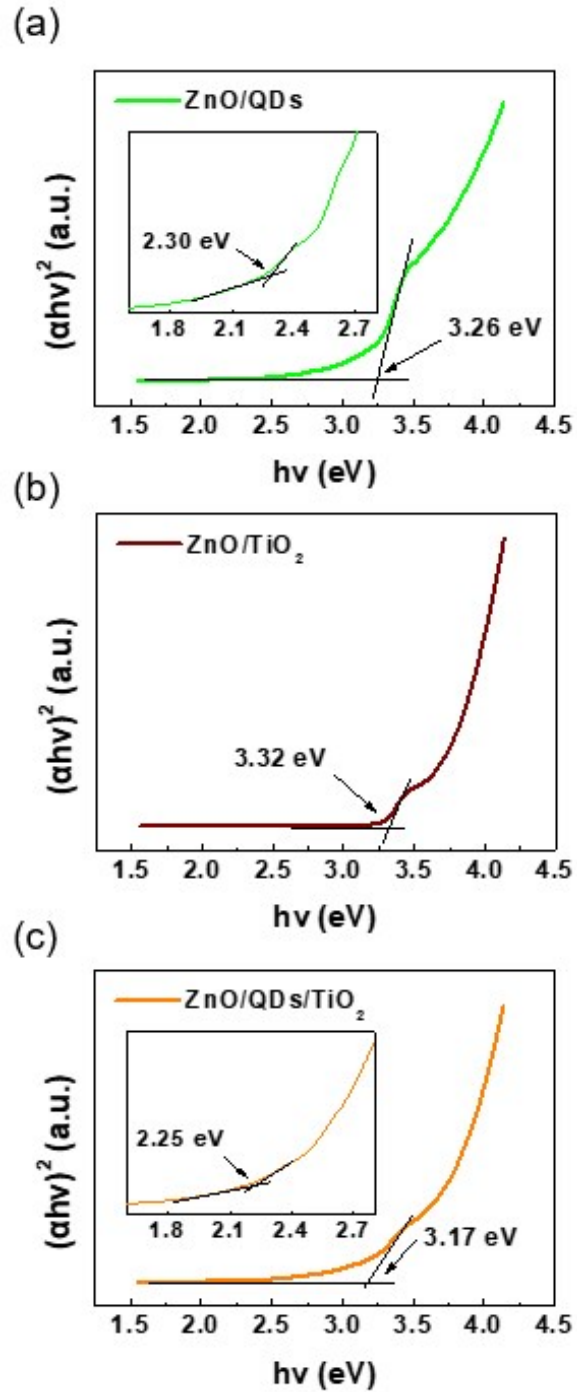


Figure S9. Tauc plots fitted by the $(\alpha h\nu)^2$ values of (a) ZnO/QDs and (b) ZnO/TiO₂, and (c) ZnO/QDs/TiO₂ film. The inset shows tauc plots with narrow ranges of each film.

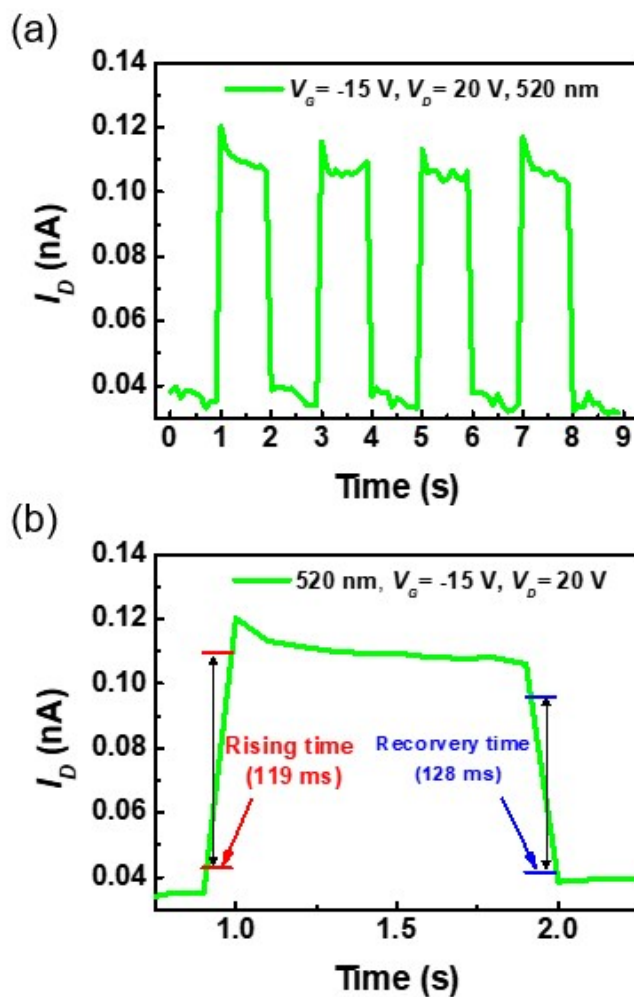


Figure S10. (a) Photo response of the ZnO/QDs TFTs and (b) Photo response characteristics of the device under periodic illumination of the wavelength ($\lambda = 520$ nm, $P = 4.5$ mW cm⁻²). Rising and falling time was defined as the interval between 10 % and 90 % of the signal.

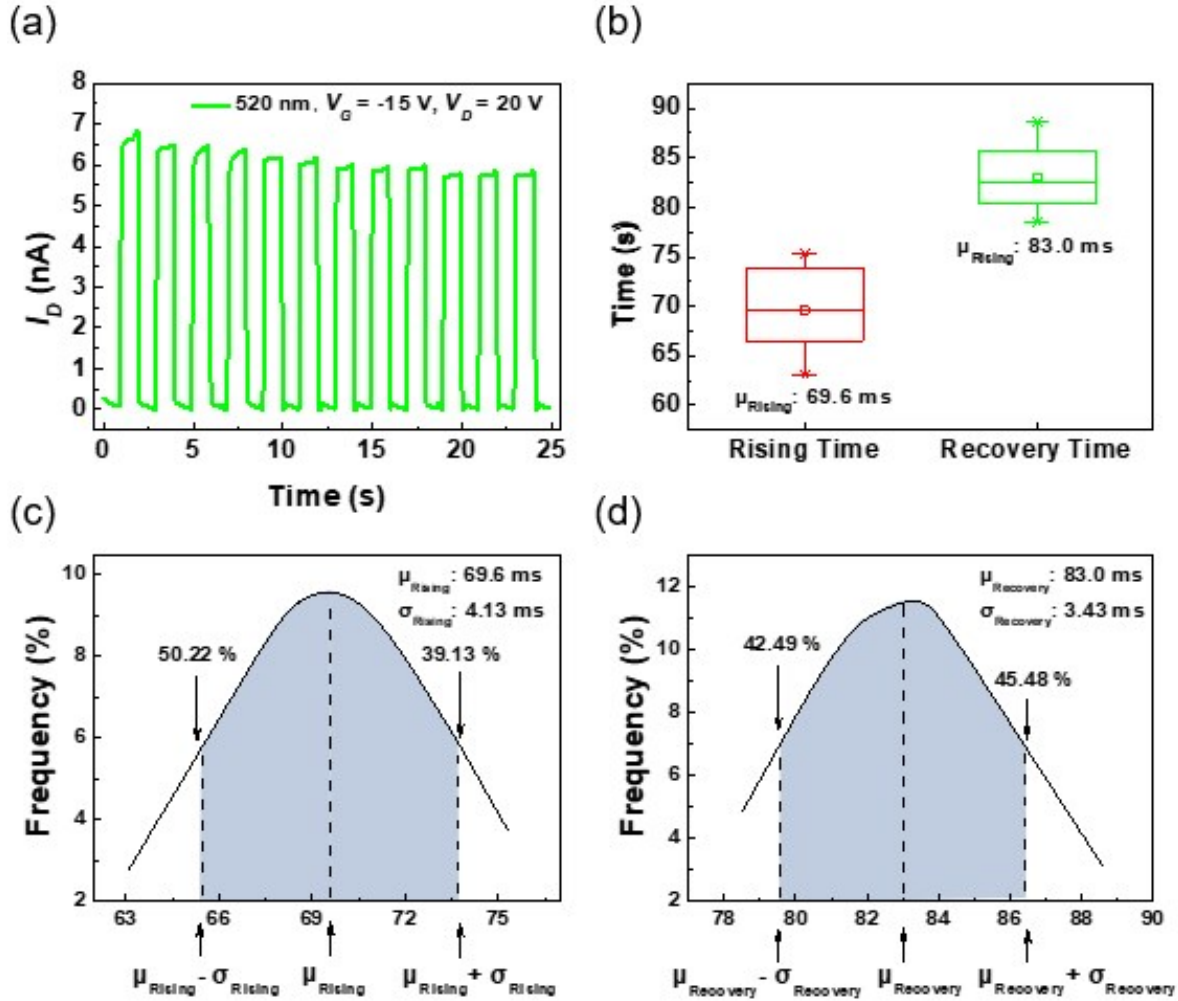


Figure S11. (a) Photo response of the ZnO/QDs TFTs under the periodic illumination of the the wavelength ($\lambda = 520 \text{ nm}$, $P = 4.5 \text{ mW cm}^{-2}$) for 25 s. (b) Error bar of rising and recovery time. The normal distributions of (c) rising and (d) recovery time. The average values are 69.6 and 83.0 ms in rising and recovery time. The deviations are 4.13 and 3.43 ms in rising and recovery time.

	a_1	t_1 [ns]	a_2	t_2 [ns]	Decay average time $\langle\tau\rangle$ [ns]
QDs	0.430	3.737	0.570	14.934	13.156
ZnO/QDs	0.332	2.307	0.668	12.457	11.602
ZnO/QDs/TiO ₂	0.902	1.954	0.098	4.623	2.500

Table S1. Fitting coefficients (a_1 , a_2 , t_1 , and t_2) and average lifetimes of the QD, ZnO/QDs, and ZnO/QDs/TiO₂ films estimated through measured TRPL decay profiles.

	$1 / t_1$ [ns ⁻¹]	$1 / t_2$ [ns ⁻¹]	Transition rate (t^{-1}) [ns ⁻¹]
QDs	0.268	0.067	0.335
ZnO/QDs	0.433	0.080	0.514
ZnO/QDs/TiO ₂	0.512	0.216	0.728

Table S2. Charge transfer rates of the QD, ZnO/QDs, and ZnO/QDs/TiO₂ films calculated through estimated TRPL decay profiles.